Kinetics of Intramolecular Electron Transfer between Phthalimide Groups Linked by $-(CH_2)_n-$ or $-(CH_2CH_2O)_mCH_2CH_2-$ Chains. Studies of Chain Flexibility

K. Shimada, Y. Shimozato, and M. Szwarc*

Contribution from the Department of Chemistry, State University of New York College of Environmental Science and Forestry, Syracuse, New York 13210.
Received March 10, 1975

Abstract: We prepared a series of radical anions having the formulas $PI(CH_2)_nPI\cdot^-$ (with n varying from 3 to 16) and $PI(CH_2CH_2O)_mCH_2CH_2PI\cdot^-$ (with m varying from 1 to 4). Here PI- denotes phthalimide residue. The frequency P of *intra*molecular electron transfer, $PI(CH_2)_nPI\cdot^- \rightleftarrows \cdot^-PI(CH_2)_nPI$ and $PI(CH_2CH_2O)_mCH_2CH_2PI\cdot^- \rightleftarrows \cdot^-PI(CH_2CH_2O)_m-CH_2CH_2PI$, was determined in five solvents for a wide range of temperatures. For the hydrocarbon chains, $-(CH_2)_n-$, the frequency P sharply decreases as n increases from 3 to 4 and 5, it reaches an undeniable minimum for $n = 6$, passes through a flat maximum for $n = 9$ or 10, and then decreases as n increases further. The nature of the investigated solvents affects only slightly the value of P; however, the frequency of exchange increases considerably with rising temperature. Substitution of $-(CH_2CH_2O)_mCH_2CH_2-$ for a hydrocarbon chain with the same number of skeleton atoms increases P by a factor of about 3, provided $m > 1$. The results are discussed in terms of static and dynamic models of the reaction, and it seems that the dynamic model accounts better for our findings than the static model. Hence, the value of P seems to reflect the rate of conformational changes of the investigated chains.

A technique permitting studies of the behavior of molecular chains was described in previous papers.[1] The method utilizes the *intra*molecular electron transfer between two α-naphthyl groups (-N) attached to the ends of a hydrocarbon chain, $-(CH_2)_n-$, as a device probing the dynamics of such molecules. The motion of the end groups affects the shape of the ESR spectra of $N-(CH_2)_n-N\cdot^-$ radical ions and, hence, from their shape, the rate, P, of the *intra*molecular electron exchange can be determined as a function of n and of the temperature of solution. For sufficiently large n ($n > 6$), $P(n + 1)^{3/2}/k_{ex}$ was found to be independent of n and of the nature of the solvent (HMPA or DME), although its value varies with temperature. Here k_{ex} refers to the bimolecular rate constant of electron exchange in the model system

$$Bu\text{-}N\cdot^- + Bu\text{-}N \xrightarrow{k_{ex}} \text{exchange}$$

We have now extended these studies utilizing *N*-phthalimide (PI) as an alternative end group and carrying out the investigation in five different solvents over a wide temperature range. We compared also the behavior of the hydrocarbon chains, $-(CH_2)_n-$, with the behavior of chains simulating polyethylene oxide, $-(CH_2CH_2O)_mCH_2CH_2-$.

Preparation of Bisphthalimides and of the Investigated Radical Ions. We prepared the compounds having the general formulas $PI(CH_2)_nPI$ and $PI(CH_2CH_2O)_mCH_2CH_2PI$ with $n = 2, 3, 4, 5, 6, 7, 8, 9, 10, 12, 14$, and 16 and $m = 1$, 2, 3, and 4, PI denoting an *N*-phthalimide moiety:

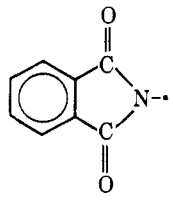

The preparation followed the method of Kolesnikov et al.,[2] and the synthesized compounds were repeatedly crystallized from toluene–methanol mixtures before being used. They melt sharply, and the respective melting points agree with the available literature data.[3] The NMR spectra in CCl_3D show the expected absorbances, and the mass spectroscopic fragmentation patterns reported elsewhere[4] confirm their structure.

The HMPA (hexamethylphosphoric triamide) solutions of the radical ions were obtained by reducing the appropriate bisimide with potassium in DME and thereafter replacing the ether by HMPA. A typical solution contained the radical ions at $\sim 10^{-4}$ *M* concentration together with a tenfold excess of the parent compound. This excess ensured the virtual absence of diradical ions in the investigated solution. The reduction of the amides in other solvents, DMF (dimethylformamide), DMAc (dimethylacetamide), DME (dimethoxyethane), and PN (propionitrile), was accomplished electrochemically, following the procedure described in the preceding paper.[5]

Knowing the kinetics of *inter*molecular electron transfer,[5] we could conclude that, under the above conditions, the *inter*molecular transfer is too slow to affect the ESR spectra, and therefore the observed variations of their shape have to be attributed to the *intra*molecular exchange.

The ESR spectra were recorded on a V4504 Varian spectrometer, the cavity being equipped with temperature controller calibrated by a Cu–constantan thermocouple.

Examination of the ESR Spectra. The ESR spectra of bisphthalimide radical ions resemble, at the very slow rate of exchange, that of the "monomer", the latter being exemplified by the spectrum of *n*-butylphthalimide$\cdot^-$ shown in Figure 1 of the preceding paper.[5] At a high rate of exchange, they acquire the shape of the ESR spectrum of a hypothetic dimer shown in Figure 1 of this paper. The latter spectrum has been computer simulated using coupling constants equal to ½ of those characterizing the spectrum of $BuPI\cdot^-$ radical ion. The shape of the computed dimer spectrum is virtually identical with that of the spectrum of $PI(CH_2)_2PI\cdot^-$ radical ion also seen in Figure 1.

The "monomer-like" spectrum is characterized by five groups of lines arising from the coupling of the electron to the N nucleus and to the two equivalent aromatic protons

having similar coupling constants as the N nucleus (for the data, see Table I of the preceding paper). The "dimer-like" spectrum (Figure 1) consists of nine groups of lines arising from the coupling of the electron to two equivalent N nuclei and the four equivalent aromatic protons having $a_H \approx a_N$ (see Figure 1 which shows both kinds of spectra).

The principles characterizing the shape of the ESR spectra of the bisimides, outlined in the preceding paragraph, are recognized in Figures 2, 3, and 4. Figure 2 depicts the spectra of the slowly exchanging $PI(CH_2)_{14}PI^{\cdot -}$ in HMPA recorded at temperatures varying from −15 to +45°. At −15°, the characteristic five groups of lines of the "monomer" are clearly perceived, although the triplets arising from the interaction with the aromatic protons 2 and 5 disappear (compare Figure 2 with Figure 1). As the rate of exchange increases with rising temperature, the larger triplets, still seen at −15° (a = 0.53 G, due to the aliphatic protons), collapse and finally disappear at 30°, whereas new lines (marked by arrows) appear at 45°. The latter signify the emergence of the dimer structure which becomes dominant at still higher rates of exchange ($P > 10^7$ sec^{-1}).

The ratios of the heights of the lines marked by arrows and seen in Figure 2 (T = −15, 0, and +15°) or in Figure 3 (T = −15 and 0°) provide a convenient measure of the rate of exchange P when P is in the range $1\text{-}7 \times 10^6$ sec^{-1}. At higher rates of exchange, the slope of the shoulder, marked by arrows in Figures 2 (T = 30°), 3 (T = 15°), and 4 (T = −15°), is sensitive to the value of P and hence it provides a method of calibration. For $P > 2 \times 10^7$ sec^{-1}, its value is gauged by the relative height of the new line attributed to the "dimer" (see Figures 2, (45°), 3 (30 or 45°), and 4 (for $T \geq 0°$)). These characteristic features of the experimental spectra are compared with those observed in the spectra simulated by computer for chosen values of P, and thus reliable values of experimental P are deduced.

Computer Simulated Spectra. In this work, as in the previous one, the method of Harriman and Maki[6] was adopted in computer simulation of the ESR spectra. The appropriate coupling constants listed in Table I of the preceding paper were used in the simulation and, for reasons explained below, $1/T_2$ was taken to be 65 mG (the width of the individual lines). The "individual" lines are in fact envelopes of the lines formed by splitting caused by the aliphatic protons 2′ and 3′. The ratio of $a_{1'}:a_{2'}:a_{3'}$ was assumed to be 2.8:0.16:0.05 by analogy with those found from the analysis of the ESR spectrum of $BuN^{\cdot -}$ radical anion,[7] and thus we arrived at $a_{2'}$ = 0.035 G and $a_{3'}$ = 0.010 G. These values were used in simulation of the envelope which gave a Lorentzian line with a width of 65 mG when $P > 0.3$ G. Some spectra were simulated with $1/T_2$ = 80 or 100 mG, but it was found that this change of $1/T_2$ does not affect the shape of the spectrum, provided that $P > 1$ G, while it considerably reduces the noise in the computation. Examples of computer simulated spectra are shown in Figure 5, where the simulated spectra are compared with the appropriate experimental ones. The calibration curves were obtained by plotting the appropriate characteristic features of the computed spectra, e.g., the earlier mentioned ratios of the peak heights, as functions of P.

Results

Our findings are summarized in Tables I to V and the dependence of the rate of exchange, P, on the number n of skeleton atoms of the chain linking the PI groups is exemplified by Figure 6 showing log P determined in HMPA plotted vs. log (n + 1). For the hydrocarbon chains, $-(CH_2)_n-$, the observed dependence is complex; P steeply decreases as n increases from 3 to 4 and 5, reaches an undeniable minimum for n = 6, passes through a flat maximum for n = 9 or 10, and then continually decreases with increasing n. Such patterns of behavior are seen in all the investigated solvents and at all studied temperatures.

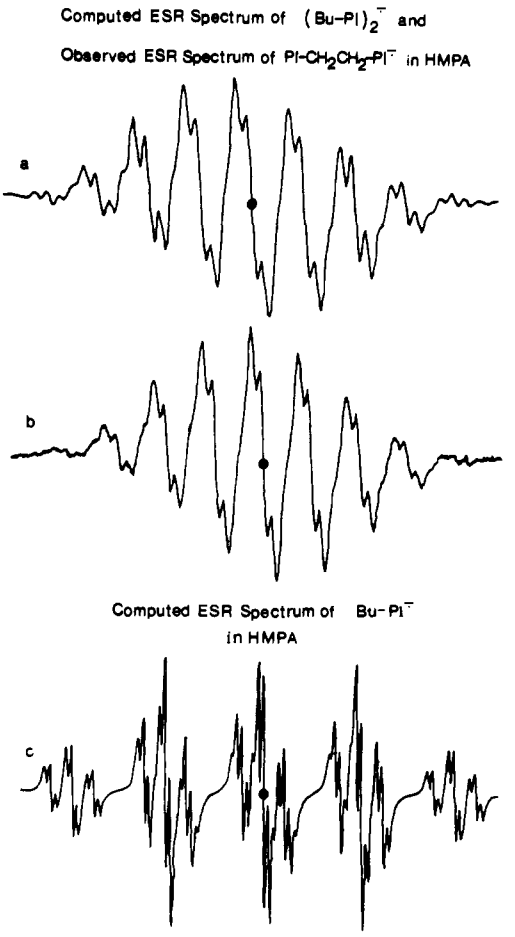

Figure 1. (a) Computed ESR spectrum of the hypothetical dimer $(-CH_2PI)_2^{\cdot -}$ in HMPA; (b) observed ESR spectrum of $PICH_2CH_2\text{-}PI^{\cdot -}$ in HMPA; (c) computed ESR spectrum of $BuPI^{\cdot -}$ in HMPA. The coupling constants of the dimer are one-half of those found for $BuPI^{\cdot -}$.

In contrast, for the oxygen containing chains, viz., $-(CH_2CH_2O)_mCH_2CH_2-$, P is only slightly affected by $n = 3m + 2$ if $m \leq 4$. For $PICH_2CH_2OCH_2CH_2PI^{\cdot -}$, the rate of exchange is approximately equal to that found for $PI(CH_2)_5PI^{\cdot -}$ if measured in the same solvent and at the same temperature. However, for M = 2, 3, and 4 (n = 8, 11, and 14, respectively), the rate of exchange is substantially higher in the $PI(CH_2CH_2O)_mCH_2CH_2PI^{\cdot -}$ system than for the hydrocarbon chains with equal number of skeleton atoms. This observation, which is evident on comparison of the spectra shown in Figures 2 and 3, is significant; it implies a higher flexibility of the oxygen-containing chains than the hydrocarbon ones.

As pointed out earlier, the bimolecular rate constant of the *inter*molecular electron transfer, $BuPI^{\cdot -} + BuPI \rightarrow$ exchange, is virtually independent of the nature of the investigated solvent. The same is found in the present study, e.g., at 0° the values of P for n = 10, 12, 14, or 16 vary in the different solvents within 30%, or less, of their average values, although larger variations are observed when n = 3, 4, or 5.

The dependence of P on temperature at constant n is illustrated by Figure 7 where the data obtained in HMPA are plotted in the Arrhenius fashion. The activation energies and the corresponding frequency factors obtained from

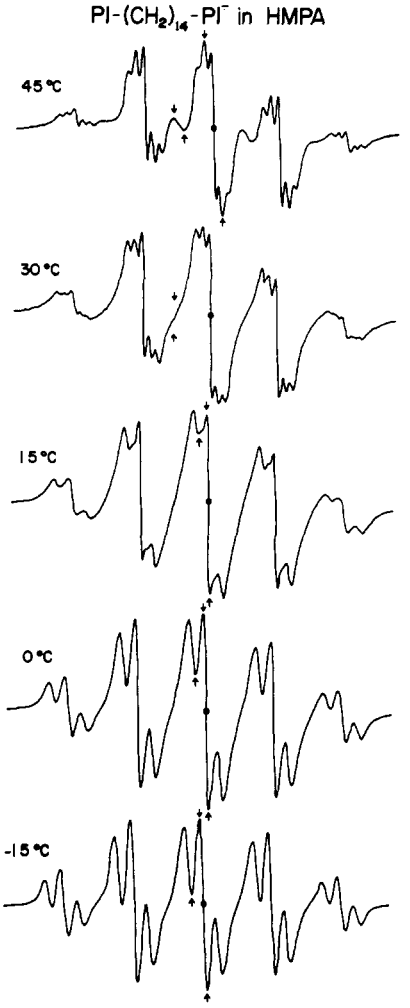

Figure 2. ESR spectra of $PI(CH_2)_{14}PI^{\cdot -}$ in HMPA at temperatures ranging from −15 to +45°.

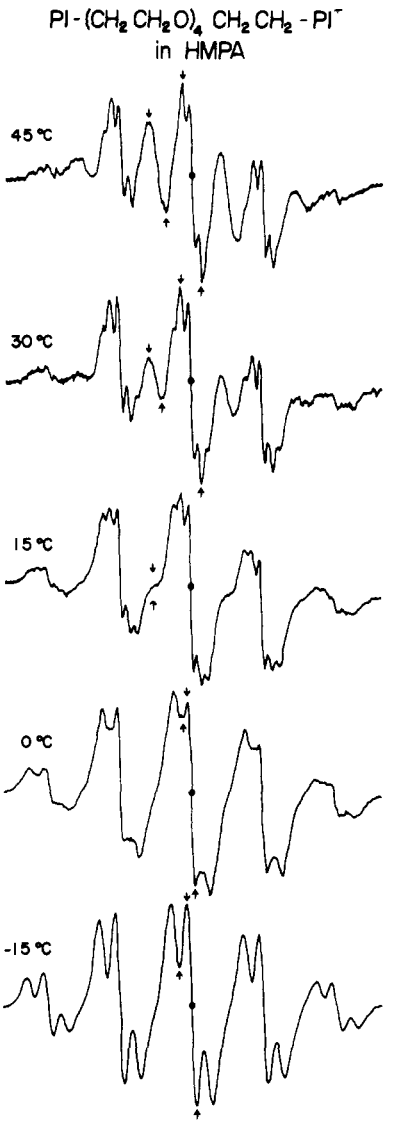

Figure 3. ESR spectra of $PI(CH_2CH_2O)_4CH_2CH_2PI^{\cdot -}$ in HMPA at temperatures ranging from −15 to +45°.

the straight lines shown in this figure are listed in Table VI. It is also interesting to note that P/k_{ex} is virtually independent of the solvent's nature when $n = 3$ or $n \geq 6$. However, the nature of solvent affects the value of P/k_{ex} for $n = 4$, and even more for $n = 5$.

Discussion

The Behavior of Long Chains. For long hydrocarbon chains ($n \geq 10$), the rate P of the *intra*molecular exchange is substantially slower for $PI(CH_2)_nPI^{\cdot -}$ and $N(CH_2)_nN^{\cdot -}$ than could be expected on the basis of the *inter*molecular exchange. This conclusion follows from examination of Table VII where we listed the ratios P/k_{ex} determined in HMPA. The ratio P/k_{ex} represents the effective concentration of the neutral group were it detached from the chain and set free to react bimolecularly with the radical ion at the rate P and with rate constant k_{ex}. The third line of each set of data gives the *minimum* concentration of the acceptor calculated on the assumption that only one, freely moving single neutral group is present in a sphere with a radius equal to the length of the *extended* chain. The comparison with the upper lines shows that the "effective" concentrations are lower, often by a factor >5, than the *minimum* concentrations. This finding demonstrates that the constraints imposed by the chain greatly hinder the rate of the observed *intra*molecular reaction.

Two factors could account for these results. The constraints of the chain might reduce the number of configurations needed for electron transfer. In other words, the probability of finding the two exchanging groups in the required configurations might be lower when they are linked by a chain than when one is free to move through a sphere of a radius equal to the length of the *extended* chain, while the other remains located at its center. For chains possessing more than ten bonds, this is unlikely, especially in view of a large reduction in the observed rate. Alternatively, a chain may hinder the movement of the exchanging groups and reduce the frequency of their encounters.

The latter suggestion needs to be elaborated. Any bimolecular solution reaction involves three steps: meeting of the reacting molecules, the actual reaction, and the separation of the products. In an exchange reaction, this scheme involves three rate constants:

$$X^{\cdot -} + X \underset{k_s}{\overset{k_d}{\rightleftarrows}} (X^{\cdot -}, X) \underset{k_t}{\overset{k_t}{\rightleftarrows}} (X, X^{\cdot -}) \underset{k_d}{\overset{k_s}{\rightleftarrows}} X + X^{\cdot -}$$

and leads to $k_{ex} = k_d k_t/(2k_t + k_s)$. Thus, for $k_t \gg k_s$ one finds $k_{ex} = \frac{1}{2}k_d$, i.e., the reaction is then diffusion controlled, whereas for $k_t \ll k_s$, the observed $k_{ex} = (k_d/k_s)k_t$. It is probable that the increase of solvent's viscosity affects to the same degree the values of k_d and k_s; it slows down the mutual approach of the reacting species but, by the same token, hinders their separation when they had approached each other. Hence, the equilibrium constant k_d/k_s

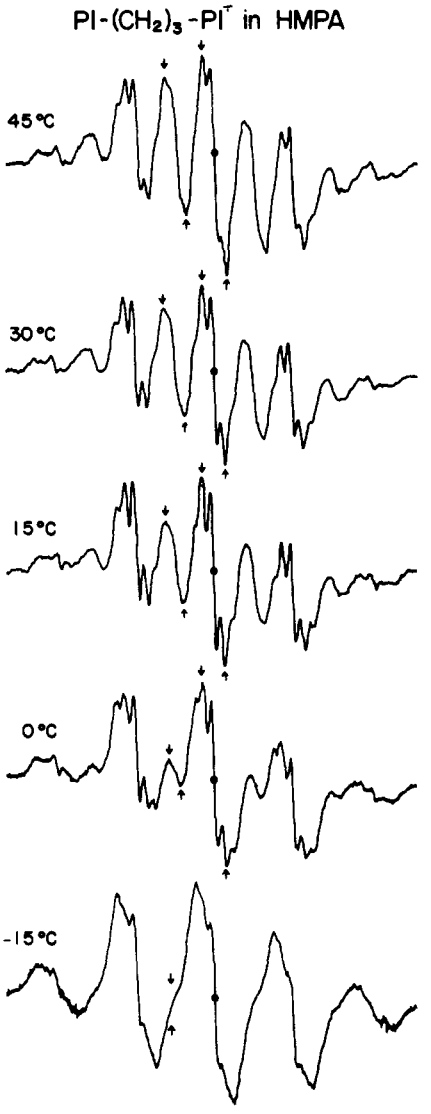

Figure 4. ESR spectra of $PI(CH_2)_3PI\cdot^-$ in HMPA at temperatures ranging from −15 to +45°.

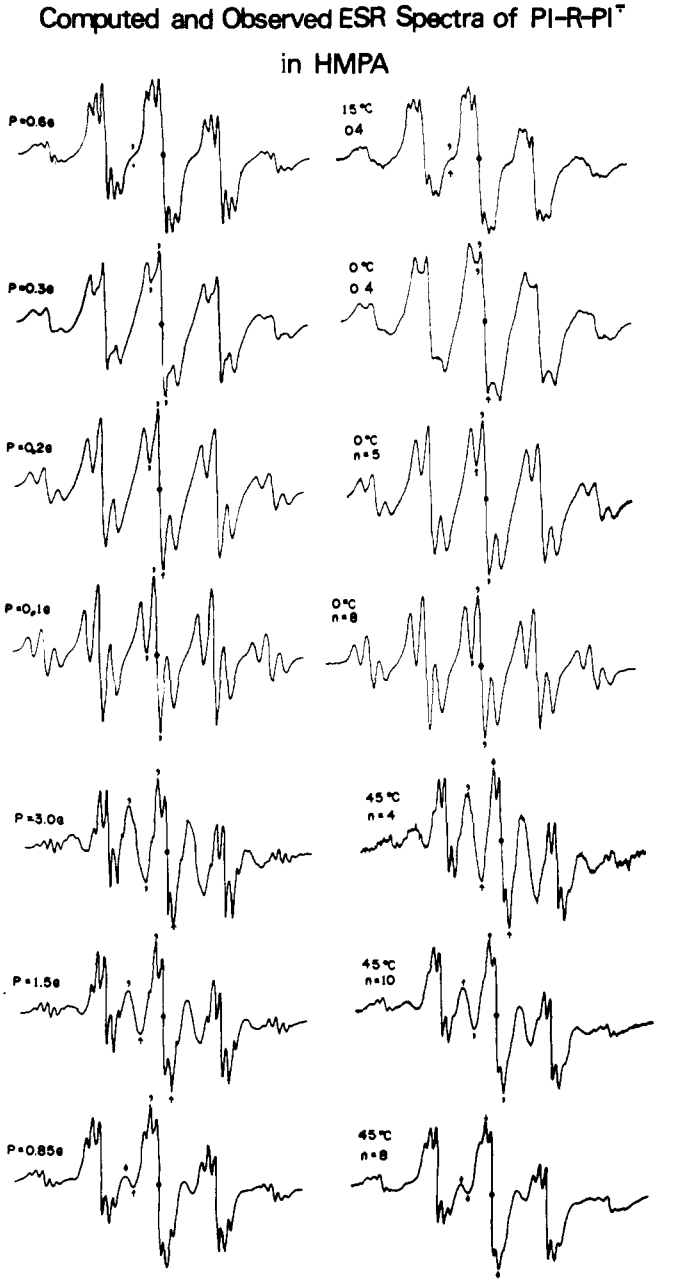

Figure 5. Computed and observed ESR spectra. Solvent HMPA. Note the changes in their shape with increasing frequency of exchange.

would be independent of the viscosity and, since k_t is not expected to be influenced by it either, the overall rate constant of the reaction should not decrease as the viscosity of the medium increases.

If the same principle applies to the *intra*molecular transfer studied in our work, then the stiffness of the chain would not affect the rate of exchange, provided the actual transfer of the electron is slower than the rate of conformational changes. Kinetics of *inter*molecular exchange reported in the preceding paper[5] indicates that k_t is somewhat smaller than k_s; i.e., the observed rate is not affected by the viscosity of the investigated solvents. Therefore, if the dynamic model implies to the investigated *intra*molecular exchange, the restrictions imposed on the motion of the end groups by the chain have to impair their mobilities to a much greater extent than the viscosity of the medium. Moreover, under such conditions, the rate of conformational changes must be *slower* than the rate of electron transfer. The rate of *intra*molecular exchange should therefore be unaffected by the viscosity of the solvent. Our findings are consistent with these conclusions, although they do not provide yet an ultimate proof for the validity of the dynamic model.

It is instructive to compare the P values of $N(CH_2)_nN\cdot^-$ and $PI(CH_2)_nPI\cdot^-$ determined for n's ≥ 10. The results obtained in HMPA, given in the last three lines of Table VIII, show that $r_n = P\{N(CH_2)_nN\cdot^-\}/P\{PI(CH_2)_nPI\cdot^-\}$ is virtually independent of n and of temperature. A static model of the reaction leads to $P = \Sigma p_i k_i$, where p_i is the probability of finding the system in configuration i, and k_i is the rate of exchange in this configuration. Hence, the static model could account for the independence of r_n on n only if the substitution of phthalimide groups for naphthyl moieties leaves p_i's unaffected and if the ratio $k_i(N)/k_i(PI)$ is independent of i. The first assumption is improbable, the distribution of *polar* phthalimides groups should be different than that of the *nonpolar* naphthyls, and both distributions should be affected to a different degree by the length of the chain. On the other hand, the dynamic model may account for the independence of r_n on n since the common rate of conformational changes is then the slowest step.

The frequency P of *intra*molecular transfer depends on the length of chain and, for longer chains, increase of its length affects the reaction in a similar way as a dilution affects a biomolecular reaction. In the previous study,[1] it was

Table I. Rate of Intramolecular Electron Exchange, P, for PIRPI· in HMPA

R	Temp, °C				
	−15	0	15	30	45
$-(CH_2)_3-$	7.4×10^6	1.8×10^7	3.9×10^7	7.5×10^7	1.4×10^8
$-(CH_2)_4-$	2.9×10^6	6.2×10^6	1.3×10^7	2.5×10^7	5.3×10^7
$-(CH_2)_5-$	1.4×10^6	3.2×10^6	6.2×10^6	1.2×10^7	2.3×10^7
$-(CH_2)_6-$	5.0×10^5	1.0×10^6	2.2×10^6	3.6×10^6	7.1×10^6
$-(CH_2)_7-$	8.9×10^5	1.8×10^6	3.7×10^6	6.2×10^6	1.3×10^7
$-(CH_2)_8-$	8.9×10^5	1.8×10^6	4.0×10^6	7.0×10^6	1.6×10^7
$-(CH_2)_9-$	1.3×10^6	3.4×10^6	5.3×10^6	1.1×10^7	2.0×10^7
$-(CH_2)_{10}-$	2.2×10^6	4.5×10^6	7.9×10^6	1.5×10^7	2.7×10^7
$-(CH_2)_{12}-$	1.9×10^6	3.8×10^6	7.0×10^6	1.3×10^7	2.3×10^7
$-(CH_2)_{14}-$	1.5×10^6	2.9×10^6	5.5×10^6	1.1×10^7	1.8×10^7
$-(CH_2)_{16}-$	1.1×10^6	2.3×10^6	4.1×10^6	7.6×10^6	1.3×10^7
$-CH_2CH_2OCH_2CH_2-$	6.3×10^5	1.6×10^6	3.8×10^6	9.7×10^6	2.1×10^7
$-(CH_2CH_2O)_2CH_2CH_2-$	1.3×10^6	2.8×10^6	7.9×10^6	1.6×10^7	3.0×10^7
$-(CH_2CH_2O)_3CH_2CH_2-$	2.4×10^6	7.0×10^6	1.3×10^7	2.8×10^7	5.2×10^7
$-(CH_2CH_2O)_4CH_2CH_2-$	2.4×10^6	7.2×10^6	1.3×10^7	3.2×10^7	6.0×10^7

Table II. Rate of Intramolecular Electron Exchange, P, for PI·⁻RPI in DMF

R	Temp, °C		
	0	20	40
$-(CH_2)_3-$	4.5×10^7	7.6×10^7	1.4×10^8
$-(CH_2)_4-$	1.5×10^7	3.1×10^7	5.1×10^7
$-(CH_2)_5-$	1.1×10^7	2.7×10^7	5.3×10^7
$-(CH_2)_6-$	3.6×10^6	6.2×10^6	1.1×10^7
$-(CH_2)_7-$	5.1×10^6	9.2×10^6	1.7×10^7
$-(CH_2)_8-$	5.2×10^6	8.9×10^6	1.6×10^7
$-(CH_2)_9-$	5.9×10^6	1.1×10^7	2.0×10^7
$-(CH_2)_{10}-$	5.8×10^6	1.1×10^7	1.9×10^7
$-(CH_2)_{12}-$	4.3×10^6	8.0×10^6	1.4×10^7
$-(CH_2)_{14}-$	3.5×10^6	6.2×10^6	1.1×10^7
$-(CH_2)_{16}-$	2.6×10^6	5.0×10^6	8.7×10^6
$-CH_2CH_2OCH_2CH_2-$	1.4×10^7	2.6×10^7	4.1×10^7
$-(CH_2CH_2O)_2CH_2CH_2-$	1.1×10^7	2.0×10^7	3.4×10^7
$-(CH_2CH_2O)_3CH_2CH_2-$	1.4×10^7	2.4×10^7	4.2×10^7
$-(CH_2CH_2O)_4CH_2CH_2-$	8.3×10^6	1.8×10^7	3.3×10^7

Table III. Rate of Intramolecular Electron Exchange, P, for PI·⁻RPI in DMAc

R	Temp, °C			
	−20	0	20	40
$-(CH_2)_3-$	1.3×10^7	2.5×10^7	4.9×10^7	1.1×10^8
$-(CH_2)_4-$	5.3×10^6	1.2×10^7	2.6×10^7	5.6×10^7
$-(CH_2)_5-$	4.1×10^6	1.1×10^7	2.2×10^7	4.4×10^7
$-(CH_2)_6-$	1.8×10^6	3.5×10^6	5.3×10^6	1.0×10^7
$-(CH_2)_{10}-$	3.0×10^6	6.2×10^6	1.1×10^7	2.0×10^7
$-(CH_2)_{12}-$	2.5×10^6	4.7×10^6	9.7×10^6	1.6×10^7
$-(CH_2)_{14}-$	1.6×10^6	3.6×10^6	6.6×10^6	1.1×10^7
$-(CH_2)_{16}-$	1.2×10^6	2.6×10^6	4.5×10^6	8.0×10^6
$-CH_2CH_2OCH_2CH_2-$	4.0×10^6	9.7×10^6	1.7×10^7	3.3×10^7
$-(CH_2CH_2O)_2CH_2CH_2-$	4.7×10^6	1.2×10^7	2.2×10^7	3.2×10^7
$-(CH_2CH_2O)_3CH_2CH_2-$	4.4×10^6	1.1×10^7	2.0×10^7	4.0×10^7
$-(CH_2CH_2O)_4CH_2CH_2-$	4.5×10^6	1.1×10^7	2.2×10^7	3.8×10^7

shown that the factor $(n + 1)^{3/2}$ accounts for this "dilution" effect. We calculated, therefore, the values of $(P/k_{ex})(n + 1)^{3/2}$ for each solvent and each temperature covered by this work, using the data for $n = 10$, 12, 14, and 16. Thus normalized values are indeed independent of n, departing by not more than 5% from their average.

The Behavior of the Short Chains. While the frequency of *intra*molecular electron transfer in the $N(CH_2)_nN^{\cdot-}$ system *monotonically* decreases with increasing n, the rate of exchange of $PI(CH_2)_nPI^{\cdot-}$ shows a pronounced minimum for $n = 6$ followed by a flat maximum at n equal 8, 9, or 10. The explanation of this difference may involve the following points.

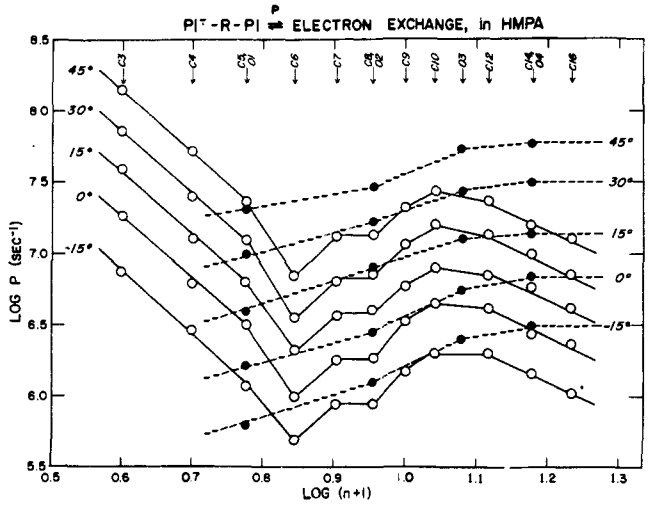

Figure 6. Dependence of the frequency of *intra*molecular electron transfer on n, the number of atoms separating the PI moieties. Solvent HMPA. (○) $PI(CH_2)_nPI^{\cdot-}$; (●) $PI(CH_2CH_2O)_mCH_2CH_2PI^{\cdot-}$.

Electron transfer from an $-N^{\cdot-}$ radical ion to an $-N$ group is rapid even at 9 Å distance,[8] as shown by the electron exchange between two naphthyl groups attached through equatorial methylenes to 1 and 4 carbon atoms of cyclohexane. In the analogous radical ions of cyclohexane with phthalimide moieties replacing naphthyl groups, the intramolecular exchange is too slow to be observed.[9] However, when the -PI's are brought closer to each other, being linked to the equatorial methylenes attached to the 1 and 3 carbons of cyclohexane, a slow exchange is observed.[9] This implies that the interaction causing the transfer is weaker in the phthalimide than in the naphthyl system. We intend, therefore, to calculate by the Monte Carlo approach the probability of finding the terminal groups of a chain involving $n + 1$ bonds at a distance d as a function of n and d and to investigate whether the variation of the latter parameter could account for our findings.

The geometry of *N*-alkylphthalimides needs clarification. Is the nitrogen atom pyramidal or planar? We believe it is planar, but no clear answer to this question is available.[10] Determination of the crystal structure of *N*-butylphthalimide may be desired.

The mutual orientation of the two reacting phthalimide groups should be also considered. Since they are polar, the antiparallel orientation of their dipoles is more favorable than the parallel one, and it is likely that the former orientation may lead to a faster electron transfer than the latter.

Table IV. Rate of Intramolecular Electron Exchange, P, for $PIRPI^{\cdot-}$ in DME

R	Temp, °C				
	−40	−20	0	20	40
$-(CH_2)_3-$	4.3×10^6	9.3×10^6	2.0×10^7	4.3×10^7	4.7×10^7
$-(CH_2)_4-$	1.8×10^6	3.2×10^6	6.0×10^6	1.1×10^7	1.5×10^7
$-(CH_2)_5-$	1.2×10^6	2.7×10^6	5.3×10^6	1.0×10^7	1.6×10^7
$-(CH_2)_6-$			1.9×10^6	3.0×10^6	5.7×10^6
$-(CH_2)_{10}-$	1.2×10^6	2.1×10^6	3.5×10^6	6.3×10^6	1.1×10^6
$-(CH_2)_{12}-$		1.8×10^6	3.0×10^6	5.0×10^6	8.0×10^6
$-(CH_2)_{14}-$		1.5×10^6	1.6×10^6	3.8×10^6	6.9×10^6
$-(CH_2)_{16}-$		1.2×10^6	1.9×10^6	3.2×10^6	5.5×10^6
$-CH_2CH_2OCH_2CH_2-$	8.7×10^5	2.3×10^6	4.8×10^6	8.8×10^5	1.9×10^7
$-(CH_2CH_2O)_2CH_2CH_2-$	1.8×10^6	2.5×10^6	5.6×10^6	1.2×10^7	2.2×10^7
$-(CH_2CH_2O)_3CH_2CH_2-$	1.2×10^6	2.8×10^6	5.4×10^6	1.2×10^7	2.1×10^7
$-(CH_2CH_2O)_4CH_2CH_2-$	1.2×10^6	2.8×10^6	5.1×10^6	8.7×10^6	1.8×10^7

Table V. Rate of Intramolecular Electron Exchange, P, for $PIRPI^{\cdot-}$ in PN

R	Temp, °C			
	−20	0	20	40
$-(CH_2)_3-$	2.9×10^7	6.5×10^7	1.5×10^8	2.6×10^8
$-(CH_2)_4-$	2.2×10^7	3.7×10^7	6.1×10^7	1.0×10^8
$-(CH_2)_5-$	1.5×10^7	3.0×10^7	5.0×10^7	8.1×10^7
$-(CH_2)_6-$		$\sim 4.5 \times 10^6$	7.0×10^7	1.8×10^7
$-(CH_2)_{10}-$			9.7×10^6	2.2×10^7
$-(CH_2)_{12}-$			7.9×10^6	2.0×10^7
$-(CH_2)_{14}-$			7.1×10^6	1.4×10^7
$-(CH_2)_{16}-$			6.2×10^6	1.3×10^7
$-CH_2CH_2OCH_2CH_2-$	1.9×10^7	3.1×10^7	4.2×10^7	4.6×10^7
$-(CH_2CH_2O)_2CH_2CH_2-$	1.2×10^7	1.8×10^7	3.1×10^7	4.3×10^7
$-(CH_2CH_2O)_3CH_2CH_2-$	1.3×10^7	1.9×10^7	3.0×10^7	4.3×10^7
$-(CH_2CH_2O)_4CH_2CH_2-$	8.8×10^6	1.5×10^7	2.3×10^7	2.8×10^7

Table VI. Activation Energies and Frequency Factors for the Intramolecular Electron Transfers in $PIRPI^{\cdot-}$ in HMPA[a]

R	E, kcal/mol	A, M^{-1} sec^{-1}
$-(CH_2)_3-$	8.1	5.0×10^{13}
$-(CH_2)_4-$	7.8	9.5×10^{12}
$-(CH_2)_5-$	7.4	3.1×10^{12}
$-(CH_2)_6-$	7.4	6.4×10^{11}
$-(CH_2)_7-$	7.4	1.2×10^{12}
$-(CH_2)_8-$	7.4	1.7×10^{12}
$-(CH_2)_9-$	7.4	1.0×10^{12}
$-(CH_2)_{10}-$	6.7	9.7×10^{11}
$-(CH_2)_{12}-$	6.7	7.8×10^{11}
$-(CH_2)_{14}-$	6.7	6.3×10^{11}
$-(CH_2)_{16}-$	6.7	4.8×10^{11}
$-CH_2CH_2OCH_2CH_2-$	9.6	7.5×10^{13}
$-(CH_2CH_2O)_2CH_2CH_2-$	8.9	3.4×10^{13}
$-(CH_2CH_2O)_3CH_2CH_2-$	8.6	4.0×10^{13}
$-(CH_2CH_2O)_4CH_2CH_2-$	8.6	4.5×10^{13}

[a] The reported activation energies are reliable within ±0.5 to ±1.0 kcal/mol.

The orientation is irrevelant in the nonpolar naphthalene system. Therefore it may be significant that the rate of *intra*molecular transfer in $N(CH_2)_3N^{\cdot-}$ is 100 times faster than in $PI(CH_2)_3PI^{\cdot-}$ (see Table VIII). The PI dipoles of this compound acquire parallel orientation when in juxtaposition—an orientation presumably required for electron transfer, and our suggestion may explain this anomaly. As the length of the chain increases, the P(N)/P(PI) ratio rapidly decreases and it reaches a low and approximately constant value of about 1.5–2 when n = 10, 12, or 16.

The unfavorable orientation of the PI groups might contribute to the high activation energies of the *intra*molecular exchange in short chain radical anions (see Table VI).

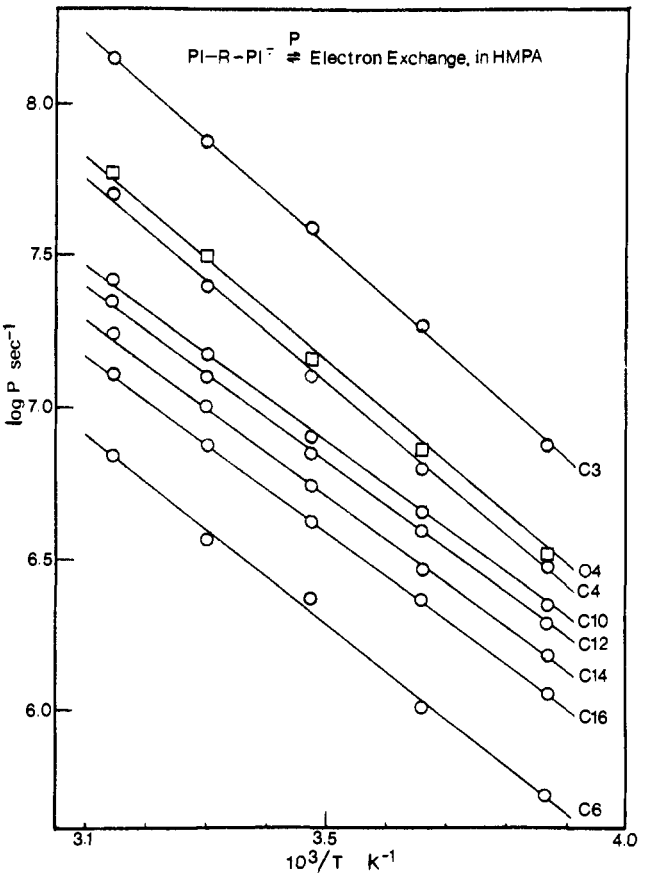

Figure 7. Temperature dependence of the frequency of *intra*molecular electron transfer in $PI(CH_2)_nPI^{\cdot-}$ at constant n's.

Table VII. P/k_{ex} for $N(CH_2)_nN\cdot^-$ and $PI(CH_2)_nPI\cdot^-$ for $n \geq 10$

		Solvent [HMPA], M				
n	R	−15 °C	0 °C	+15 °C	30 °C	45 °C
10	N−	0.040	0.053	0.047	0.055	0.057
	PI−	0.022	0.025	0.029	0.036	0.041
	Ex ch[a]	0.155	0.155	0.155	0.155	0.155
12	N−	0.033	0.037	0.037	0.050	0.045
	PI−	0.019	0.021	0.026	0.031	0.035
	Ex ch[a]	0.094	0.094	0.094	0.094	0.094
14	N−					
	PI−	0.015	0.016	0.020	0.026	0.027
	Ex ch[a]	0.061	0.061	0.061	0.061	0.061
16	N−	0.020	0.023	0.022	0.022	0.024
	PI−	0.011	0.013	0.015	0.018	0.020
	Ex ch[a]	0.042	0.042	0.042	0.042	0.042
20	N−	0.013	0.018	0.015	0.014	0.011
	PI−					
	Ex ch[a]	0.022	0.022	0.022	0.022	0.022

[a] Extended chain. Concentration for 1 molecule in a sphere of radius = the length of extended chain.

Table VIII. The Ratio $P[N(CH_2)_nN\cdot^-]/P[PI(CH_2)_nPI\cdot^-]$

	Solvent HMPA				
n	−15 °C	0 °C	15 °C	30 °C	45 °C
3	95	142	172	173	136
4	55	53	56	100	83
5	28	11	12	12	11
6	36	23	20	18	10
8	12	10	7	6	4
10	1.8	2.1	1.6	1.5	1.4
12	1.7	1.8	1.4	1.6	1.3
16	1.8	1.8	1.5	1.2	1.2

However, these relations are complex, and the treatment developed in our earlier paper[11] seems pertinent to this problem.

Comparison of $PI(CH_2)_nPI\cdot^-$ and $PI(CH_2CH_2O)_m$-$CH_2CH_2PI\cdot^-$. The rate of *intra*molecular electron transfer is about three times faster for $PI(CH_2CH_2O)_4CH_2CH_2$-$PI\cdot^-$ than for $PI(CH_2)_{14}PI\cdot^-$, although in both radicals the interacting groups are separated by 14 atoms. This difference may arise either from the more compact nature of the oxygen-containing chain when compared with the polymethylene one or from higher *dynamic* flexibility of the former than of the latter. Compactness of a chain may be measured by its characteristic ratio, $\langle r^2\rangle_0/nl^2$ (the symbols used here have their conventional meaning[12]). Studies of polyoxyethylene oligomers and polymers[12] indicate that this ratio is lower by a factor of about 1.5 for the oxygen-containing oligomers (n = 15) than for the equivalent polymethylenes, but later work[13,14] suggests that the characteristic ratio for the polyoxyethylene oligomers is higher than reported earlier. If both oligomers were equally compact, our findings would imply that the *dynamic* flexibility of the oxygen-containing chains is higher by about a factor of three than that of the polymethylenes. This observation, compatible with the known mechanical behavior of polyoxyethylenes and polyethylenes, suggests that our approach provides information about *dynamic* flexibility of molecular chains.

Final Conclusions

Two models may account for the progress of *intra*molecular reactions: a dynamic and a static one. The former applies only to reactions which are sufficiently fast, while the latter accounts for the slow reactions. A special situation is created when the reacting groups are crowded together in a way which favors the attainment of transition state. In such a system, the reaction may be unusually fast, even faster than expected when the calculation is based on the pertinent bimolecular rate constant and the concentration of the reagent corresponding to its bulk concentration (the highest physically possible concentration). Formation of anhydride[14] with the simultaneous displacement of alkoxy group from the anion depicted below may serve as an outstanding example of such a process.

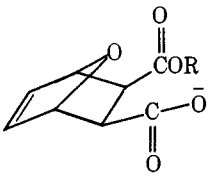

The static model is inherently associated with the concept of effective concentration of the reagent C_{eff}. The chain forces the interacting groups to remain in the vicinity of each other and thus speeds up the reaction. It should be stressed, however, that the static model can never lead to the inequality $C_{eff} < C_{min}$ where $C_{min} = 1000/V_{max}N$, V_{max} being the volume of a sphere with radius equal to the length of extended chain. The dynamic model may account for the above inequality,[17] and therefore our findings favor the dynamic model for the studied *intra*molecular electron transfer.

Values of C_{eff} shed light on the problem of distribution of chain conformations provided that the rate of change of conformations is much faster than the rate of reaction. An example is provided by a recent work of Winnik and his colleagues.[15] Using a previously developed model,[16] they calculated the probability of finding a reactive CH_2 group in the vicinity of a carbonyl group of an excited benzophenone. Such a group quenches then the phosphorescence of benzophenone. The rate constants of *intra*- and *inter*molecular quenching were determined experimentally, and their ratio was compared with the calculated probability p divided by volume v available to the quenching group when locked in the interacting configuration. The ratio p/v represents the previously defined effective concentration, C_{eff}. The agreement between the calculated p/v and the observed P/k_{inter} demonstrates therefore that the configurations of the hydrocarbon chains are those expected for flexible chains randomly oriented in the investigated solution, subject to the condition that trans conformers are favored by 0.5 kcal/mol over the gauche conformers.

Acknowledgment. It is a pleasure to acknowledge the finanical support of these studies by the donors of the Petroleum Research Fund, administered by the American Chemical Society, and by the National Science Foundation.

References and Notes

(1) (a) H. D. Connor, K. Shimada, and M. Szwarc, *Macromolecules*, **5**, 801 (1972); (b) K. Shimada and M. Szwarc, *J. Am. Chem. Soc.*, **97**, 3313 (1975).
(2) G. S. Kolesnikov, O. Y. Fedotova, and V. V. Trezvov, *Zh. Prikl. Khim.* (Leningrad), **42**, 2639 (1969).
(3) R. H. F. Manske, *J. Am. Chem. Soc.*, **51**, 1202 (1929); A. W. Baldwin, *J. Chem. Soc.*, 2947 (1929); A. Muller and E. Feld, *Monatsh. Chem.*, **58**, 12 (1931); A. W. Baldwin and R. Robinson, *J. Chem. Soc.*, 1264 (1934); G. Venags, *Ber. Dtsch. Chem. Ges. B*, **75**, 719 (1942); F. P. Dwyer, N. S. Gill, E. C. Grafas, and F. Lions, *J. Amer. Chem. Soc.*, **75**, 1526 (1953); W. C. Austin, M. D. Potter, and E. P. Taylor, *J. Chem. Soc.*, 1489 (1958).
(4) Y. Shimozato, K. Shimada, and M. Szwarc, *Org. Mass Spectrosc.*, in press.
(5) Y. Shimozato, K. Shimada, and M. Szwarc, *J. Am. Chem. Soc.*, the preceding paper in this issue.
(6) J. E. Harriman and A. H. Makl, *J. Chem. Phys.*, **39**, 778 (1963).
(7) E. de Boer and C. MacLean, *Mol. Phys.*, **7**, 191 (1965).

(8) K. Shimada and M. Szwarc, *Chem. Phys. Lett.* **28**, 540 (1974).
(9) K. Shimada, Y. Shimozato, and M. Szwarc, *Chem. Phys. Lett.*, **31** (1975).
(10) A. Arcoria, J. Barassin, and H. Lumbroso, *Bull. Soc. Chim. Fr.*, 2509 (1964).
(11) K. Shimada and M. Szwarc, *J. Am. Chem. Soc.*, **97**, 3321 (1975).
(12) J. E. Mark and P. J. Flory, *J. Am. Chem. Soc.*, **88**, 3702 (1966).
(13) Dr. J. E. Mark, private communication.
(14) D. R. Beech and C. Booth, *J. Polymer Sci., Part A-2*, **7**, 575 (1969).
(15) (a) M. A. Winnik, C. K. Lee, S. Basu, and D. S. Saunders, *J. Am. Chem. Soc.*, **96**, 6182 (1974); (b) M. A. Winnik, D. S. Saunders, S. N. Basu, and C. K. Lee, *ibid.*, in press.
(16) (a) M. A. Winnik, R. E. Trueman, G. Jackowski, D. S. Saunders, and S. G. Whittington, *J. Am. Chem. Soc.*, **96**, 4843 (1974); (b) M. A. Winnik, D. S. Saunders, and S. G. Whittington (this manuscript in preparation describes the method of calculation which accounts for the different energies of trans and gauche conformations).
(17) Of course, for sufficiently long chains, C_{elf} becomes smaller than C_{min} even in the dynamic model of the reaction. This, however, does not affect our argument.

Thermal Isomerization Reactions of *cis*-9,10-Dihydronaphthalene Derivatives

Leo A. Paquette* and Michael J. Carmody

Contribution from the Evans Chemical Laboratories, The Ohio State University, Columbus, Ohio 43210. *Received February 4, 1975*

Abstract: *cis*-9,10-Dihydronaphthalene-*2,3-d*$_2$ (**37**) rearranges upon heating in the gas phase (510°, contact time ~1 sec) to return the starting tetraene frame carrying near statistical distribution of the isotopic label at all positions. The propensity for degenerate behavior in **37** thereby established, the response of the 9,10-dicarbomethoxy (**3**) and 9,10-dimethyl derivatives (**26**) to thermal activation was also studied. When heated in dimethoxyethane solution at 80° (19 hr), **3** afforded predominantly 1,5- and 1,9-dicarbomethoxy-*cis*-9,10-dihydronaphthalene (**12** and **13**). Hydrocarbon **26** behaved analogously, giving rise to the structurally isomerized (but with retention of the *cis*-9,10-dihydronaphthalene framework) 1,5- and 1,9-dimethyl isomers **29** and **30**. The consequences of heating each of these six compounds at higher temperatures were also studied. Quite complex product mixtures were seen. Considerably more elucidative were the kinetic data for rearrangement of **3** and **26**. From the findings that both compounds isomerize with comparable activation parameters ($E_a \approx 26$ kcal/mol; log $A \approx 12$; $\Delta H^{\ddagger} \approx 25$ kcal/mol; and $\Delta S^{\ddagger} \approx -4$ eu), the conclusion is reached that comparable reaction pathways are followed in the two cases. The possible involvement of intramolecular Diels–Alder and Cope rearrangement pathways could be readily discounted. Rather, conclusions are reached that passage to 1,9 products proceeds via [1,5]suprafacial migration of one of four identical trigonal α carbons, while conversion to the 1,5 isomers involves transient intervention of *cis*^{5}-cyclodecapentaene intermediates. The agreement between the present data and past findings with prototypical reaction channels of these types is discussed.

Degenerate rearrangement reactions occupy a unique position among the myriad types of thermal isomerization. That certain molecules can suffer appreciable levels of bond cleavage only to possess the latent capability for interchange of their constituent atoms and ultimate reconstruction of the starting frames merits recognition as a fascinating reactivity pattern. Since the much publicized demonstration of this behavior in bullvalene,[1] several additional examples of related fluxional isomerism have been uncovered. In the main, the $(CH)_n$ class of hydrocarbons has been primarily responsible for developments in this field. For example, the capacity for degenerate isomerization is now recognized for bicyclo[4.2.2]decatetraene,[2] snoutene,[3] hypostrophene,[4] cyclooctatetraene,[5] semibullvalene,[6] and lumibullvalene.[7]

Within this group of compounds, the mechanisms which allow for attainment of degeneracy are recognized to vary widely, but some pathways, such as that followed by *cis*-9,10-dihydronaphthalene (**1**), have remained elusive.[8] As a direct consequence of the possibility that thermal activation of **1** may result in valence isomerization to *cis*^{5}-cyclodecapentaene (**2**), there has been a strong undercurrent of interest in this system for some time.[9] All attempts to achieve

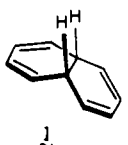

1

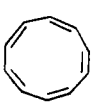

2

disrotatory thermal ring expansion of **1**,[10] its 9,10-dicarbomethoxy derivative,[11] and 12-oxa[4.4.3]propellatetraene[12] to such 10π-electron systems have failed. With Masamune's recent successful low-temperature synthesis of **2**[13] has come the realization that the lability of [10]annulenes precludes their isolation from thermolysis reactions. However, their transient formation under these conditions is not discounted and it was of interest to examine closely this question.

Prior to the start of this investigation, van Tamelen and Pappas had reported in 1963 that heating of dilute carbon tetrachloride solutions of **1** for 10–15 min at 150–220° resulted in quantitative conversion to naphthalene.[10] Under these conditions, therefore, aromatization with liberation of hydrogen is kinetically dominant. In view of the exceptional hydrogen transfer properties of **1**,[14] the absence of disproportionation products is rather surprising.

A year later, Vogel, Meckel, and Grimme[11] considered the possibility that replacement of the sp^3-bound hydrogens in **1** by carbomethoxyl groups as in **3** would preclude dehydrogenation and [1,5]sigmatropic hydrogen shifting from competing with the desired isomerization. These investigators noted that when **3** was heated at 90° for 2 hr and the resulting mixture of rearranged diesters directly dehydrogenated at 150°, diesters **4**–**6** were isolated together with other unidentified products. The formation of **4** and **5** was taken as an indication of the transient intervention of an unstable [10]annulene. On the other hand, the isolation of **6** has been widely interpreted[9a,c] as the probable result of intramolecular ($_{\pi}4_s + {}_{\pi}2_s$) addition to give **7** followed by retrograde Diels–Alder ring opening in the opposite direction.